TRANSPORT PROBLEMS 2019 Volume 14 Issue 3
PROBLEMY TRANSPORTU DOI: 10.20858/tp.2019.14.3.1

Keywords: gearbox; transmission; contact, mesh stiffness

Paulius BOGDEVIČIUS*, Marijonas BOGDEVIČIUS, Olegas PRENTKOVSKIS
Vilnius Gediminas Technical University
Saulėtekio al. 11, Vilnius, 10223, Lithuania
**Corresponding author*. E-mail: paulius.bogdevicius@gmail.com

INVESTIGATION OF DYNAMIC PROCESSES IN A GEARBOX WITH DEFECTS

Summary. The article presents theoretical research of a transmission system that allows examination of the dynamic processes evaluating different sizes of defects in gear tooth (0%, 20%, 50%, 80% of teeth width) and gaps between the connection of the gear teeth. The dynamics of the transmission is described using the finite element method and discreet elements. This paper presents and analyzes the results of mathematical experiments on this system.

1. INTRODUCTION

A gearbox is widely used as one of the main transmission elements in industrial and military applications to transmit power. Gear or gear teeth surfaces in particular excessively wear because of the difficult shape of the geometry caused by intense loads in transmission systems. The contact area of two connecting gear teeth is variable, causing defects in gear teeth. Defects, such as gear tooth cracks, fractures, and chipping, increase vibration levels and generate noise simultaneously as the gearbox continues to work. Early fault detection might be crucial to stop incoming systems failure.

At present, increasingly more investments are being made in the field of diagnostics. Many scientists perform mathematical modeling of defects to understand their impact on system dynamic characteristics. For example, Mohammed *et al.* [1] studied the gear system using three different dynamic models from 6 to 12 degrees of freedom (DOF) evaluating different crack sizes and pinion's displacements. The results of the first model show visible differences from other models that were made more realistic, including simulation of motor and load. From the second model, the influence of the friction on inter tooth could be seen. Jia *et al*. [2] for the object took 26 DOF transmission system which includes three shafts and two connected spur gears. This model is developed by calculating torsional stiffness and tooth load adding spalling and crack damage. For simulation, Matlab Simulink software tool was used. Patrick *et al* [3] focused on the identification of cracks in a planetary gear system using vibration sensors. Mathematical model results are compared with experiments from the results obtained from a helicopter. Using the same vibration signal modeling, *Liang et al*. [4] identified the exact gear tooth crack location. The presented results can help identify defects and it can be used as a tool for planetary gear system diagnostics. Group of researchers, Ma *et al.* [5] conducted a dynamic investigation of cracked gear systems. The whole research focused on 3 major important factors: crack propagation prediction, mesh stiffness calculation, and vibration response calculation. For the object they took three different gears. Tian *et al*. [6] carried out a model-based gear dynamic analysis and simulation research evaluating cracks' propagation level. The results suggested that the root mean square is a better statistical indicator than the Kurtosis indicator to reflect the crack propagation in the early stages.

Finite element modeling (FEM) is one of the methods to simulate gears with defects dynamic behavior; however, these models have large amount of DOF. Therefore, it becomes quite difficult to proceed with the modeling. Nevertheless, Parker *et al*. [7] proposed a nonlinear tooth contact and mesh stiffness variation model using FEM. Pruerter *et al.* [8], with the same gear teeth contact model, indicated that uneven loading on the teeth was because of differing constraints on the two sides of the teeth compared to the experimental results. Lin *et al.* [9] studied 3D dynamic contact problems. According to the results, mesh stiffness results were the same as those obtained from the conventional methods. Secondly, the case of initial speed impact is considered; the contact time is independent of the initial speed. Third, the impact time depends on the geometric parameters of the gear drive and the total contact force is proportional to the initial speed and transmission load.

To insure lifetime of the gear, stiffness calculation is one of the key parameters that is being studied by the scientists. Xue *et al.* [10] presented work on torsional stiffness evaluation in involute spur planetary gears in mesh using FEM. The theoretical gear contact position was determined using an ANSYS APDL software. Walha et al. [11] investigated the dynamics of a two-stage gear system involving backlash and time-dependent mesh stiffness. To satisfy some conditions, nonlinear dynamic systems were linearized to a linear dynamic system and each system was solved using Newmark iterative algorithms. A hypoid gear pair was taken as an object in the research carried out by Wang et al. [12]. Nonlinear mesh stiffness results showed that the increase in the mean mesh stiffness ratio tends to worsen the dynamic response amplitude and stiffness parameters have an impact on dynamic responses. Saxena et al. [13], in the mesh stiffness model, included sliding friction and spalling defects.

In this paper, dynamic teeth coupling investigation with mesh and contact stiffness defects in a gearbox system is presented. Teeth of each gear are self-contained and may have defects. The deformation of each tooth is evaluated. The size of gear tooth's stiffness defect is presented and expressed as a percentage (0, 20, 50, and 80 %). Transmission with an idle with no external excitation reveals the presence of gaps between contacting two gear teeth 50μm. The torsional vibrations of shafts and bending vibrations of gear teeth are simulated using finite and discrete elements methods.

2. MATHEMATICAL MODEL OF TRANSMISSION SYSTEMS

A mathematical model of a transmission system is considered (Fig 1.). The transmission system includes an asynchronous electrical motor, a gearbox, and connection shafts. The main parameter of the electric motor is the moment of inertia I_1, rotation angle φ_1, and torque M_{mot}. The gearbox includes two connected gear pairs, where is the evaluated moment of inertia I_2, I_3, I_4, I_5, rotational angles φ_2, φ_3, φ_4, φ_5, and gear Pitch radius R_2, R_3, R_4, R_5. For torsional rotation, only gear tooth mass is evaluated. The transmission system is unloaded (torque of resistance is equal zero, $M_{resist} = 0$).

To evaluate the rotation of the transmission elements, a mathematical model suggested by Aladjev [14] may be used:

$$\dot{M}_{mot} + d_v M_{mot} = c_v(\omega_0 - \dot{\varphi}_1) \qquad (1)$$

where M_{mot} is the rotation moment of the asynchronous electric motor; $d_v = S_v \omega_t$, $c_v = \dfrac{2M_v \cdot \omega_t}{\omega_{V0}}$ are the parameters of the electric motor; ω_0 is an angular velocity of idle running; $\dot{\varphi}_1$ is an angular velocity of the electric motor, S_v and M_v - glide and torque, ω_t - angular velocity of the motor, ω_{V0} - ideal angular velocity of the asynchronous motor.

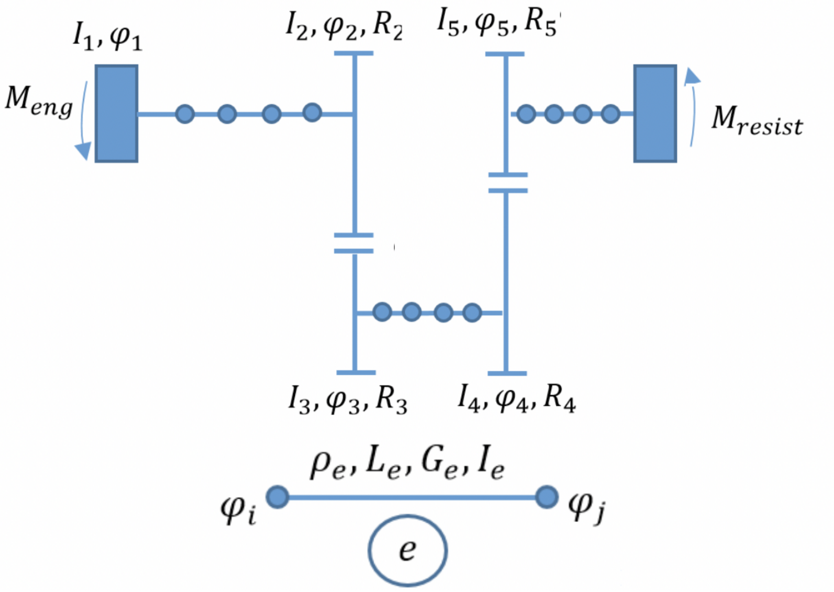

Fig. 1. Dynamic model of the transmission system

The system of equations of a rotating shaft has been considered applying the finite element method:

$$[M_e]\{\ddot{\varphi}_e\}+[C_e]\{\dot{\varphi}_e\}+[K_e]\{\varphi_e\}=\{M_e\} \quad , \tag{2}$$

where $[M_e],[C_e]$, and $[K_e]$ are the mass, damping, and stiffness matrix, respectively; $\{\ddot{\varphi}_e\},\{\dot{\varphi}_e\}$, and $\{\varphi_e\}$ are the vectors of acceleration, velocity, and displacement, respectively; and $\{M_{ie}\}$ is the vector of torques.

Rotational angle φ in the finite element is equal to:

$$\varphi=[N\{\zeta)]\{\varphi_e\}; \tag{3}$$

$$[N\{\zeta)]=[1-\zeta,\zeta], \tag{4}$$

where $\{\varphi_e\}$ is the vector of angles; $[N\{\zeta)]$ is a matrix of shape functions; and $\zeta=\frac{x}{Le}$ is a local coordinate.

Mass, stiffness, and damping matrices of the finite element of the transmission system are equal to:

$$[M_e]=\int_0^1 \rho_e I_{pe} L_e [N]^T [N] d\zeta \, , \tag{5}$$

$$[K_e]=\int_0^1 \frac{G_e I_{pe}}{L_e}\left[\frac{dN}{d\zeta}\right]^T\left[\frac{dN}{d\zeta}\right]d\zeta \, , \tag{6}$$

$$[C_e]=\alpha_e[M_e]+\beta_e[K_e] \quad , \tag{7}$$

where ρ_e is the shaft material density; I_{pe} is the polar moment of inertia, G_e is the shear module; and α_e and β_e are optional coefficients by Aladjev [14].

To evaluate the interaction of possible cracks on tooth's surface mesh stiffness, it is important to determine the size of the defect. In this model, index k indicates gear or index i - gear tooth.
The bending stiffness with a defect of the k-th gear and the i-th tooth is described by the formula:

$$k_{ki}=(1-D_{k,i})k_{ki,0} \quad , \tag{8}$$

where $D_{k,i}$ is the size of the defect $0 \le D_{k,i} \le 1$,

$$D_{k,i} = \frac{E_D}{E} \frac{(L - L_D)^3}{L^3}; \tag{9}$$

where L_D is the defect depth and L is the tooth thickness, E, E_D are the moduli of elasticity of the tooth without and with a defect

$k_{ki,0}$ is the stiffness coefficient of the i-th tooth without a defect.

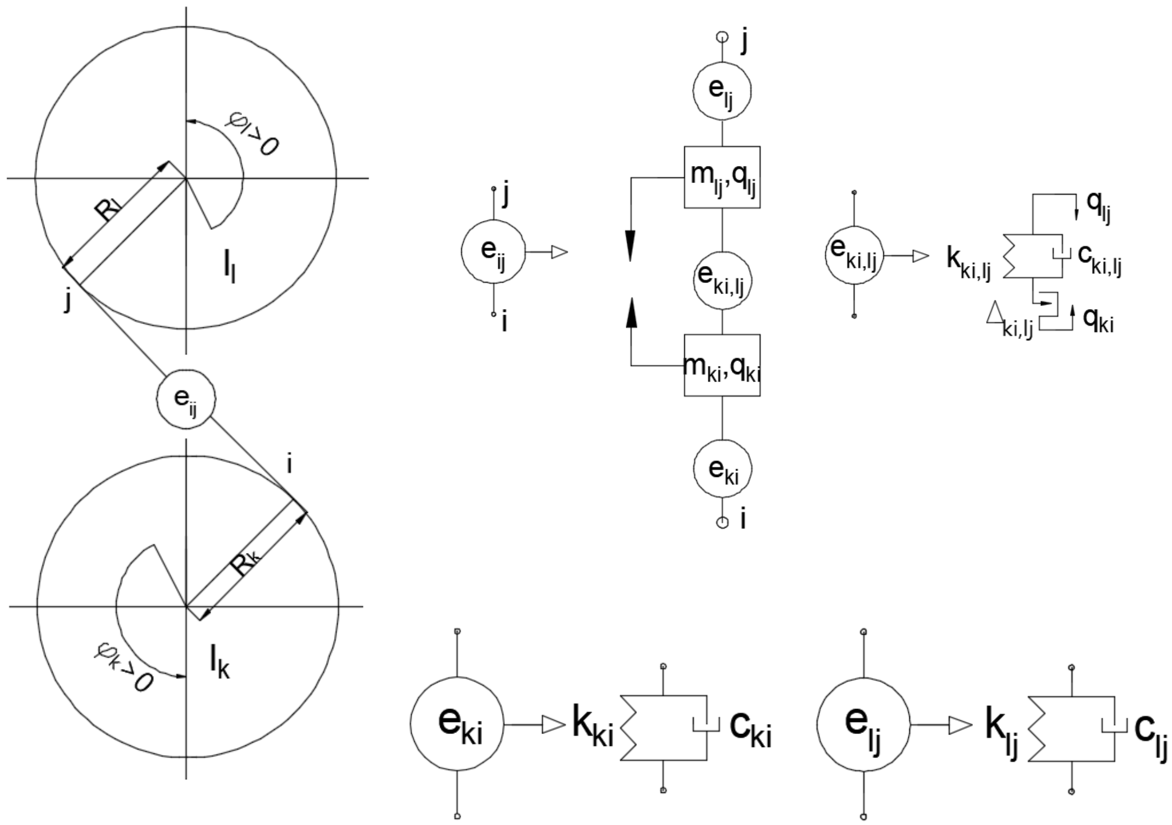

Fig. 2. Two connected gears dynamic model

The contact force by Hertzs theory between i tooth k gear and j tooth l gear is equal to:

$$F_{ki,lj} = k_{ki,lj} \left|\delta_{ki,lj}\right|^n \left(1 + \frac{3}{4}\left(1 - e^2\right) \frac{\dot{\delta}_{ki,lj}}{\dot{\delta}_{\max}}\right) H\left(\delta_{ki,lj}\right) = \left(\left(k_{ki,lj} \left|\delta_{ki,lj}\right|^n\right) + c_{ki,lj}(\delta_{ki,lj})\dot{\delta}_{ki,lj}\right) H\left(\delta_{ki,lj}\right) \tag{10}$$

,

where $k_{ki,lj}, c_{ki,lj}$ is the stiffness and the dumping coefficient between contact; n is the nonlinear power exponent determined from material and geometric properties; and $\delta_{ki,lj}$ is penetration, $\delta_{ki,lj} = q_{ki} + q_{lj} - \Delta_{ki,lj}$, where: q_{ki} and q_{lj} are the displacement vectors, $\Delta_{ki,lj}$ is the gap between two connected gear teeth, e is the restitution coefficient, and $H\left(\delta_{ki,lj}\right)$ is the Heaviside function.

The potential energy of k-th gear i-th tooth and l-th gear j-th tooth is equal to:

$$E_{p,ki} = \frac{1}{2} k_{ki} (R_k \varphi_k - q_{ki})^2; \tag{11}$$

$$E_{p,lj} = \frac{1}{2} k_{lj} (R_l \varphi_l - q_{lj})^2, \tag{12}$$

where R_k, R_l and φ_k, φ_l are base radii and rotation angles of the k-th and l-th gears, respectively, and k_{ki} and k_{lj} are the stiffness coefficients of the k-th and l-th gears, respectively.

The dissipation functions of k-th gear i-th tooth and l-th gear j-th tooth are equal to:

$$\Phi_{p,ki} = \frac{1}{2} c_{ki} (R_k \dot{\varphi}_k - \dot{q}_{ki})^2 ; \tag{13}$$

$$\Phi_{p,lj} = \frac{1}{2} c_{lj} (R_l \dot{\varphi}_l - \dot{q}_{lj})^2 , \tag{14}$$

where c_{ki} and c_{lj} are the damping coefficients.

The equations of rotation k-th gear and motion of i-th tooth area described below:

$$I_k \ddot{\varphi}_k = M_{k,trans} - \sum_{i=1}^{nzk} (k_{ki} R_k (R_k \varphi_k - q_{ki}) + c_{ki} R_k (R_k \dot{\varphi}_k - \dot{q}_{ki})), \tag{15}$$

$$m_{ki} \ddot{q}_{ki} = k_{ki} (R_k \varphi_k - q_{ki}) + c_{ki} (R_k \dot{\varphi}_k - \dot{q}_{ki}) + F_{ki,lj} s_{mesh,ki,lj} , \tag{16}$$

and l-th gear and j-th tooth are equal to:

$$I_l \ddot{\varphi}_l = M_{l,trans} - \sum_{i=1}^{nzl} (k_{lj} R_l (R_l \varphi_l - q_{lj}) + c_{lj} R_l (R_l \dot{\varphi}_l - \dot{q}_{lj})), \tag{17}$$

$$m_{lj} \ddot{q}_{lj} = k_{lj} (R_l \varphi_l - q_{lj}) + c_{lj} (R_l \dot{\varphi}_l - \dot{q}_{lj}) + F_{lj,ki} s_{mesh,ki,lj} , \tag{18}$$

where I_k, I_l are inertia moments; $M_{k,trans}$, $M_{l,trans}$ are k-th and l-th gear torques; m_{ki}, m_{lj} are mases of k-th gear i-th tooth and l-th gear j-th tooth, respectively; nzk and nzl are the numbers of gear teeth; $s_{mesh,ki,lj}$ is the parameter that takes into account the coupling of the k-th gear i-th tooth and the l-th gear j-th tooth , and $s_{mesh,ki,lj} = \left\{ \begin{matrix} 1, & is \quad coupling \\ 0, & is\ not \quad coupling \end{matrix} \right\}$. In the annex A, the derivation of the stiffness coefficient of gear is presented.

3. RESULTS AND DISCUSSION

3.1. Initial data of the research

The purpose of this research is to determine the dynamic characteristics (velocity, acceleration, torque) because of the effect of different sizes of the defect 20 %, 50 % and 80 % of whole width on tooth surface with 50μm gap between gear teeths.

Initial conditions of the variables: initially, the torque of the asynchronous electro motor, vectors of rotation angles, and angular velocity are equal ($M_{mot}(t=0) = \frac{c_v}{d_v}\left(\omega_0 - \dot{\varphi}_0\right)$, $\{\varphi(t=0)\} = 0, \left\{ \frac{d\varphi(t=0)}{dt} \right\} = \left\{ \dot{\varphi}_0 \right\}$). The number of first and third gears is equal, $nz = 30$; the number of second and fourth gears is equal, $nz = 20$. The integration time step is $\Delta t = 10 \cdot 10^{-6} s$ and the simulation time is 5 s. The data of the transmission system are shown in Tab 1.

3.2. Results and discussion of the transmission system

The dynamical characteristics of the transmission system may alter due to defects in gear tooth. The developed model of transmission with teeth defects allows a detailed analysis of the dynamic characteristics of a transmission system. The gap between two connected gears is 50 μm.

Dependencies in time of asynchronous electric motor torque and angular velocity of gear1 and gear 2 are shown in Fig. 4 when the defect size is 80%. With such defects, clearance, and idle rotation, pulsations of the torque of the electric motor appear $M_{mot}(t \geq 0,6s) \neq 0$.

Table 1

Data calculation of the transmission system

Definition	Notation	Definition	Notation
Base radius of the gear	$R_2 = 65,5 \cdot 10^{-3} m$	Mass of inertia	$I_2 = 50 \cdot 10^{-3} kg \cdot m^2$
	$R_3 = 45,5 \cdot 10^{-3} m$		$I_3 = 40 \cdot 10^{-3} kg \cdot m^2$
	$R_4 = 65,5 \cdot 10^{-3} m$		$I_4 = 50 \cdot 10^{-3} kg \cdot m^2$
	$R_5 = 45,5 \cdot 10^{-3} m$		$I_5 = 40 \cdot 10^{-3} kg \cdot m^2$
Poisson's ratio	$Pu = 0,30$	Young's modulus	$E = 210 \cdot 10^9 Pa$
Gear tooth mass	$m = 50 \cdot 10^{-3} kg$	Stiffness coefficient of teeth	$k_i = 150 \cdot 10^6 N/m$
Shaft shear modulus of rigidity	$G = 79,3 \cdot 10^9 Pa$	Damping coefficient of teeth	$c_i = 1,0 \cdot 10^{-2} Ns/m$
Shaft density	$\rho = 7820 kg/m^3$	Shaft diameter	$d_{\max} = 50 \cdot 10^{-3} m$
Shaft parameter 1	$\alpha = 1 \cdot 10^{-4}$	Shaft parameter 2	$\beta = 1 \cdot 10^{-3}$
Restitution coefficient	$e = 0,60$	Grade indicator	$n = \frac{3}{2}$

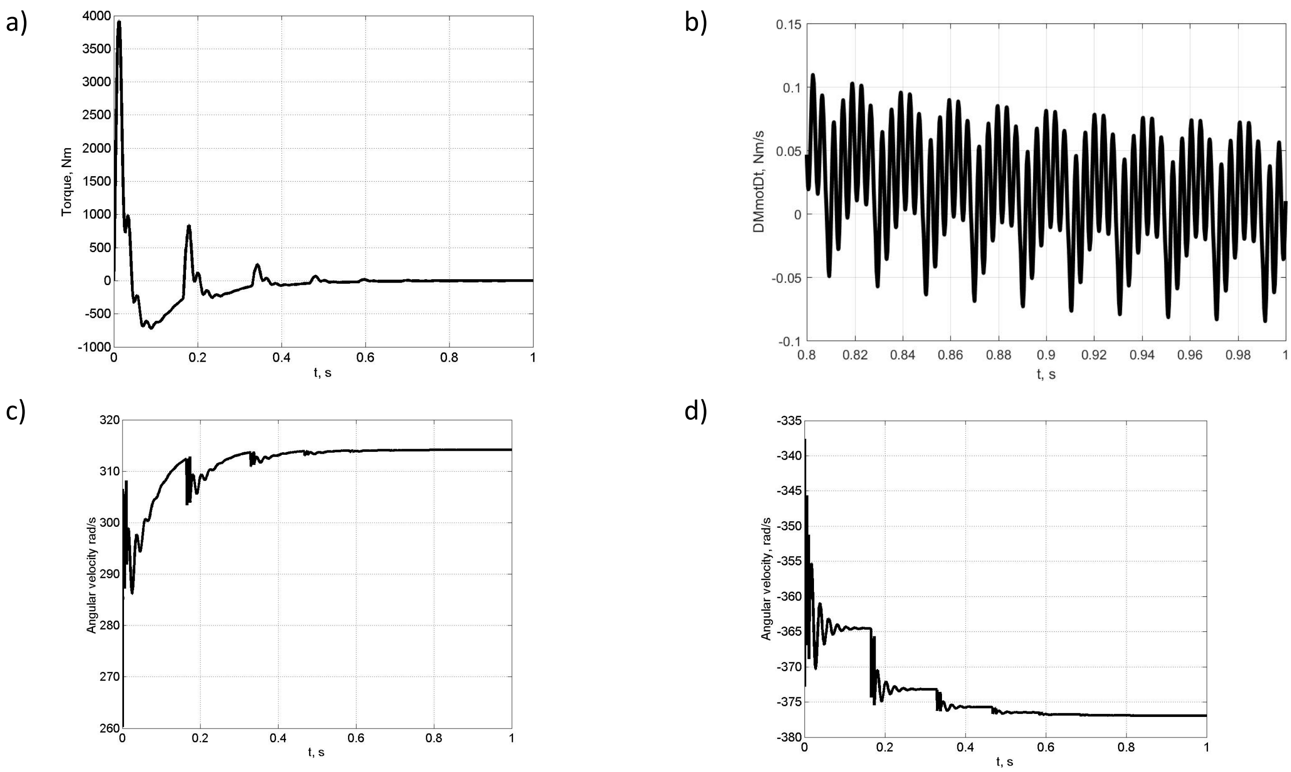

Fig. 3. Asynchronous electro motor torque and angular velocity of gear 1 and gear 2 dependencies in time: a) torque; b) Asynchronous electro motor torque derivation in time; c) angular velocity of gear 1; and d) angular velocity of gear 2

Fig. 3 shows the transmission process that remains at 0.5 s. Gear 1 angular velocity reaches 314 rad/s and gear 2 angular velocity reaches 376 rad/s. Dependencies in time of Angular acceleration of gear 1 damaged tooth 1 with different sizes of the defect are shown in Fig. 4.

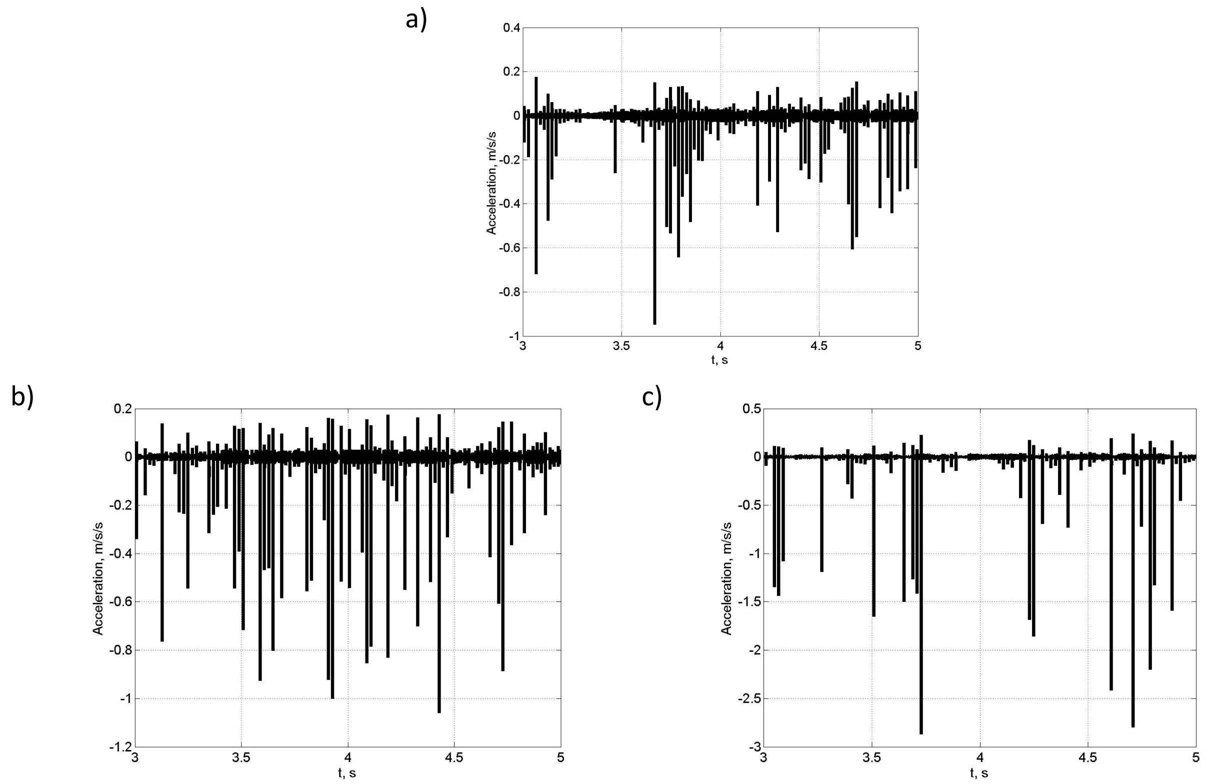

Fig. 4. Acceleration of gear 1, tooth 1 with different sizes of defect dependencies in time: a) 0%, $(D_{1,1}=0)$; b) 20% $(D_{1,1}=0,2)$; c) 50% $(D_{1,1}=0,5)$

Fig. 4 shows that acceleration changes due to an increase in the size of the defect. In the graphic, when there are no defects in the gear tooth system, the maximum value of the acceleration reaches 0,95 m/s^2. On changing the defect size to 20% and 50%, acceleration increases to 1,05 m/s^2 and 2,85 m/s^2.

When there are gaps between the teeth 50 μm and the various defects of the first tooth of the first gear wheel, torsional vibrations of the shafts and bending vibrations of the teeth are generated in the transmission. Fig. 4 shows that complex torsional vibrations occur in the transmission.

When simulating the operation of the transmission for 5s at idle rotation, the transmission does not have torsional vibrations of the elements. Therefore, it can be argued that when an alternating rotating moment of resistance is applied in the transmission, the torsional vibrations of the transmission of the elements will be more complex.

Angular acceleration of four gears dependency on frequency is shown in Fig. 5 when the size of the defect is 50%.

The four graphs in Fig. 5 show that when a defect occurs, the resonant frequency at the first gear is visible. First gear vibration by coupling is transferred to the second gear, but decreases at the third gear, which connected to the second one by the shaft and completely disappears with in fourth gear. This analysis makes it possible to determine which gear has the defect, but it does not allow us to determine which gear tooth is damaged. This is done by another spectrum analysis of the gear teeth with different defect sizes and this is shown in Fig 6.

According to Fig. 6, because of the effect of different defect sizes, the rotational frequency decreases with the maximum amplitude value. Tooth without defect $(D_{1,1}=0)$, maximum amplitude value is 220 rad/s^2 at 20000Hz frequency, when 20% $(D_{1,1}=0,2)$ value is 190 rad/s^2 at 19 000Hz frequency, at

50% $(D_{1,1} = 0,5)$ is 460 rad/s^2 18000Hz frequency and at 80% $(D_{1,1} = 0,8)$ maximum amplitude value 88 rad/s^2 at 8500Hz frequency.

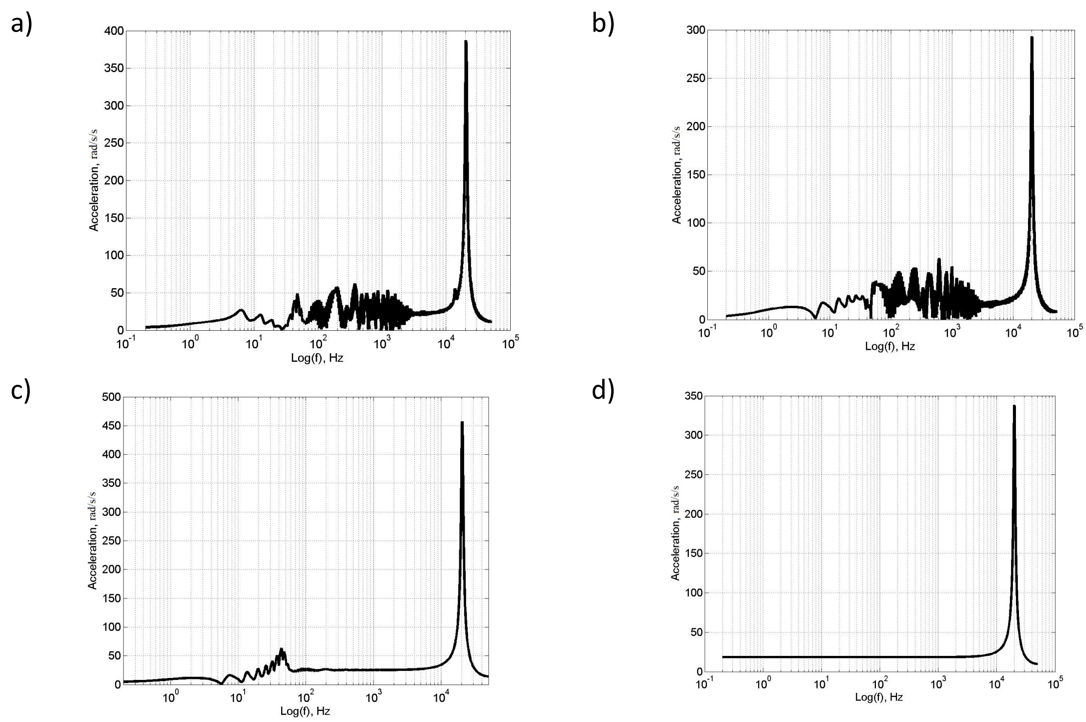

Fig. 5. Angular acceleration dependency of frequency of four gears: a) gear 1; b) gear 2; c) gear 3; and d) gear 4

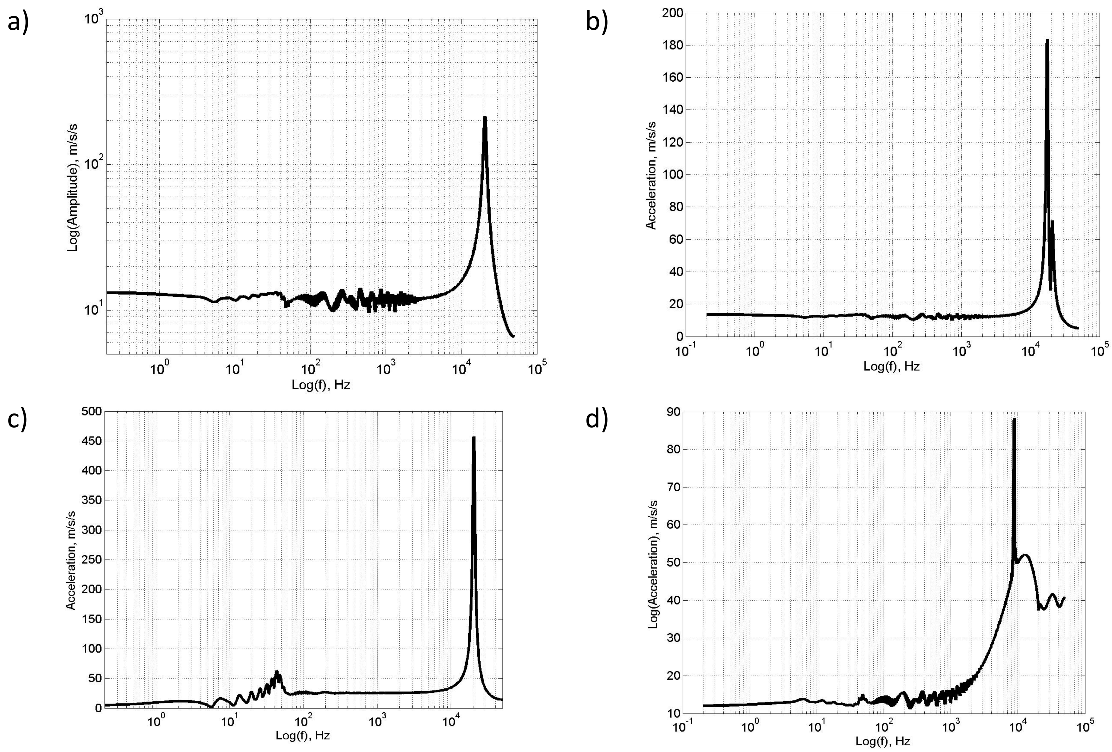

Fig. 6. Gear 1, tooth 1 acceleration dependency of frequency with the different sizes of the defect: a) 0% $(D_{1,1} = 0)$; b) 20% $(D_{1,1} = 0,2)$; c) 50% $(D_{1,1} = 0,5)$; d) 80% $(D_{1,1} = 0,8)$

4. CONCLUSION

A mathematical model of transmission system is established that allows the analysis of dynamic processes evaluating different sizes of defects on gear tooth (0%, 20%, 50%, and 80% of tooth) and gaps between connections of the gear teeth 50μm. The resonance frequency changes to a different size of defect. The bigger the size of the defect, the smaller the stiffness, and the resonance frequency decreases. Within 50% of the defect of tooth, gear 1 angular velocity reaches 314 rad/s and gear 2 angular velocity reaches 376 rad/s.

In a system without defects of the first tooth on gear 1 $(D_{1,1} = 0)$, the maximum acceleration value of the first tooth reaches 0,95 m/s^2, when the defect size is 20% $(D_{1,1} = 0,2)$, acceleration of 1 tooth increases to 1,05 m/s^2, and when the defect size is 50% $(D_{1,1} = 0,5)$, acceleration reaches 2,85 m/s^2.

To study the torsional vibrations of the transmission of elements and bending vibrations of the teeth of gear wheels with defects and gaps, the developed software has been developed.

References

1. Mohammed, O.D. & Rantatalo, M. & Aidanpἂἂ, J.-O. Dynamic modelling of a one-stage spur gear system and vibration-based tooth crack detection analysis. *Mechanical Systems and Signal Processing.* 2015. Vol. 54-55. P. 293-305.
2. Jia, S. & Howard, I. Comparison of localised spalling and crack damage from dynamic modelling of spur gear vibration. *Mechanical Systems and Signal Processing.* 2006. Vol. 20. P. 332-349.
3. Patrick, R. & Ferri, A. & Vachtsevanos, G. Effect of planetary gear carrier-plate cracks on vibration spectrum. *Journal of Vibration and Acoustics.* 2012. Vol. 134. 061001-061001-12.
4. Liang, X. & Zuo, M. J. & Hoseini, M.R. Vibration signal modeling of a planetary gear set for tooth crack detection. *Engineering Failure Analysis.* 2015. Vol. 48. P. 185-200.
5. Ma, H. & Zeng, J. & Feng, R. & et al. Review on dynamics of cracked gear systems. *Engineering Failure Analysis*. 2015. Vol. 55. P. 224-245.
6. Tain, Z. & Zuo, M.J. & Wu, S. Crack propagation assessment for spur gears using model-based analysis and simulation. *Journal of Intelligent Manufacturing*. 2012. Vol. 23. P. 239-253.
7. Parker, R.G. & Agashe, V. & Vijayakar, S.M. Dynamic response of a planetary gear system using a finite element/contact mechanics model. *Journal of Mechanical Design*. 1991. Vol. 122. P. 304-310.
8. Prueter, P.E. & Parker, R.G. & Cunliffe, F. A study of gear root strains in a multi-stage planetary wind turbine gear train using a three dimensional finite element/contact mechanics model and experiments. In: *Proceedings of the Design Engineering Technical Conference.* 2011. P. 621-633.
9. Lin, T. & Ou, H. & Li, R. A finite element method for 3D static and dynamic contact/impact analysis of gear drives. *Computer Methods in Applied Mechanics and Engineering.* 2007. Vol. 197. P. 1716-1728.
10. Xue, S. & Entwistle, R. & Mazhar, I. & Howard Ian. The torsional stiffness of involute spur planetary gears. In: *Proceedings of the 9th IFToMM International conference on Rotor Dynamics.* 2015. Vol 21. P. 1369-1378.
11. Walha, L. & Fakhfakh, T. & Haddar, M. Nonlinear dynamics of a two-stage gear system with mesh stiffness fluctuation, bearing flexibility and backlash. *Mechanism and Machine theory*. 2009. Vol. 44. P. 1058-1069.
12. Wang, J. & Lim, T.C. Effect of tooth mesh stiffness asymmetric nonlinearity for drive and coast sides on hypoid gear dynamics. *Journal of Sound and Vibration.* 2009. Vol. 319. P. 885-903.
13. Saxena, A. & Parey, A. & Chouksey, M. Time varying mesh stiffness calculation of spur gear pair considering sliding friction and spalling defects. *Engineering Failure Analysis*. 2016. Vol. 70. P. 200-211.
14. Aladjev, V. & Bogdevicius, M. *Maple: programming, physical and engineering problems*. Palo Alto: Fultus Publishing. 2006.

Annex A

The fundamental equation for structural analysis, based on the Euler beam theory, is presented where one point is fixed; the force–load behavior can be described by:

$$[K]\{u\} = \{F\},$$

where $[K]$ is the stiffness matric; $\{u\}$ is the displacement vector $\{u\}^{-T} = [q_1, \theta_1, q_2, \theta_2]$, and $\{F\}$ is the aggregated force vector.

$$\begin{bmatrix} k_{11} & k_{12} & k_{13} & k_{14} \\ k_{21} & k_{22} & k_{23} & k_{24} \\ k_{31} & k_{32} & k_{33} & k_{34} \\ k_{41} & k_{42} & k_{43} & k_{44} \end{bmatrix} \begin{Bmatrix} q_1 \\ \theta_1 \\ q_2 \\ \theta_2 \end{Bmatrix} = \begin{Bmatrix} F_1 \\ M_1 \\ F_2 \\ M_2 \end{Bmatrix}.$$

When the first point of the beam is fixed $(q_1, \theta_1) = 0$ the equation lightens:

$$\begin{bmatrix} k_{33} & k_{34} \\ k_{43} & k_{44} \end{bmatrix} \begin{Bmatrix} q_2 \\ \theta_2 \end{Bmatrix} = \begin{Bmatrix} F_2 \\ M_2 \end{Bmatrix}.$$

Then

$$k_{43}q_2 + k_{44}\varphi_2 = M_2;$$

$$\varphi_2 = k_{44}^{-1}(M_2 - k_{43}q_2);$$

$$k_{33}q_2 + k_{34}k_{44}^{-1}(M_2 - k_{43}q_2) = F_2;$$

$$[k_{33} - k_{34}k_{44}^{-1}k_{43}]q_2 = F_2 - k_{34}k_{44}^{-1}M_2;$$

$$k_{tooth}q_2 = F_{tooth}.$$

Fig. 7 shows a simplified model of a localized gear tooth of irregular shape evaluating an involute curve.

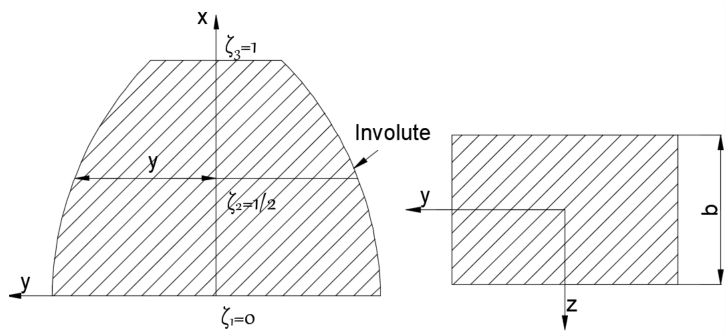

Fig. 7. Cutting contour of gear tooth

The mesh stiffness of the gear tooth is equal to:

$$k_{ij} = \int_0^1 E\left(\frac{\partial^2 N_i}{\partial\zeta^2 L_e^2}\right)\left(\frac{\partial^2 N_j}{\partial\zeta^2 L_e^2}\right) y^2 A L_e d\zeta, \; i, j = 3, 4,$$

where E is the modulus elasticity of defected gear tooth; N_i and N_j are shape functions of the beam element, y is the y coordinate, L_e is the height of the tooth; and A is the cross section area of the tooth that depends on the y coordinate. The y coordinate of the cross section of the tooth is approximated by 3 points

$$y(\zeta) = P_1(\zeta)y_1 + P_2(\zeta)y_2 + P_3(\zeta)y_3,$$

where P_i is the i-th shape function. The shape functions P_i are equal to:

$$P_1(\zeta) = 2\zeta^2 - 3\zeta + 1\,,\ P_2(\zeta) = 4\zeta(1-\zeta)\,,\ P_3(\zeta) = \zeta(2\zeta - 1)\,.$$

Then, the cross-section area of tooth A is equal to:

$$A(\zeta) = A_1 P_1(\zeta) + A_2 P_2(\zeta) + A_3 P_3(\zeta)\,,$$

A_1, A_2, A_3 are the cross section areas of a tooth at the point $\zeta_1, \zeta_2, \zeta_3$, respectively.

Then

$$k_{ij} = \int_0^1 \frac{E}{L_e^3} \left(\frac{\partial^2 N_i}{\partial \zeta^2} \right) \left(\frac{\partial^2 N_j}{\partial \zeta^2} \right) y^2(\zeta) A(\zeta) d\zeta\ ,\ i, j = 3,4\,.$$

Received 31.05.2018; accepted in revised form 20.08.2019